Biochemical and Biophysical Research Communications 407 (2011) 92–97

Contents lists available at ScienceDirect

Biochemical and Biophysical Research Communications

journal homepage: www.elsevier.com/locate/ybbrc

A novel Rieske-type protein derived from an apoptosis-inducing factor-like (AIFL) transcript with a retained intron 4 induces change in mitochondrial morphology and growth arrest

Yasuhiko Murata, Isao Furuyama, Shoji Oda, Hiroshi Mitani *

Department of Integrated Biosciences, Graduate School of Frontier Sciences, University of Tokyo, 5-1-5 Kashiwanoha, Kashiwa, Chiba 277-8561, Japan

ARTICLE INFO

Article history:
Received 23 February 2011
Available online 2 March 2011

Keywords:
AIFL
Rieske domain
Pyr_redox domain
[2Fe–2S] cluster
Intron retention

ABSTRACT

Apoptosis-inducing factor-like (AIFL) protein contains a Rieske domain and pyridine nucleotide-disulfide oxidoreductase (Pyr_redox) domain that shows 35% homology to that of apoptosis-inducing factor (AIF) protein. We identified a novel major transcript of the medaka (*Oryzias latipes*) AIFL gene that retained intron 4 (AIFL-I4) in embryos and tissues from adult fish. The product of this transcript, AIFL-I4 protein, lacked the Pyr_redox domain because of a nonsense codon in intron 4. Both AIFL-I4 and full-length AIFL (fAIFL) transcripts were highly expressed in the brain and late embryos, and relative fAIFL and AIFL-I4 expression levels differed among tissues. Transient expression of AIFL-I4 and fAIFL tagged with GFP showed that AIFL-I4 localized in the nucleus, while fAIFL localized throughout the cytoplasm. We also found that overexpression of AIFL-I4 induced a change in mitochondrial morphology and suppression of cell proliferation. AIFL-I4 mutant with a lesion in [2Fe–2S] cluster binding site of the Rieske domain did not induce these phenotypes. This report is the first to demonstrate nuclear localization of a Rieske-type protein translated from the AIFL gene. Our data suggested that the [2Fe–2S] cluster binding site was essential for the nuclear localization and involved in mitochondrial morphology and suppression of cell proliferation.

© 2011 Elsevier Inc. All rights reserved.

1. Introduction

Apoptosis-inducing factor-like (AIFL) was discovered as a human gene homologous to apoptosis-inducing factor (AIF) [1,2]. AIF, AIF-like mitochondrion-associated inducer of death (AMID, also designated p53-responsive gene 3 (PRG3)) and AIFL contain a pyridine nucleotide-disulfide oxidoreductase domain (Pyr_redox), respectively, and only AIFL of these proteins has a Rieske domain [1–5]. Xie et al. [2] has reported that full-length human AIFL and the segment containing the Rieske domain induced caspase-dependent apoptosis and localized to the mitochondria, whereas the segment containing Pyr_redox domain appeared diffuse cytoplasmic distribution and did not contribute to the pro-apoptotic function and the localization. Therefore, the Rieske domain contained in human AIFL was necessary for mitochondrial localization, but a known mitochondrial localization sequence is not contained in this domain.

Proteins with Rieske domains, which are electron transfer domains that contain [2Fe–2S] clusters, are members of the iron-sulfur cluster protein group [6]. Generally, the [2Fe–2S] cluster contained in a Rieske domain consists of two cysteines and two histidines ([2Fe–2S] cluster binding site) in the following sequence motif: Cys-X-His-$X_{15\text{-}47}$-Cys-X-X-His [7,8]. Proteins containing Rieske domains are classified into two categories: Rieske proteins and Rieske-type proteins. Rieske proteins are required for the cytochrome bc_1/b_6f complex in the aerobic respiratory chain and for photosynthesis. In addition to the two cysteines and two histidines, three amino acids (underlined) in this consensus sequence, Cys-X-His-X-Gly-Cys-$X_{12\text{-}44}$-Cys-X-Cys-His, are uniformly conserved in all Rieske proteins [8,9]. Rieske-type proteins, including AIFL, do not contain any uniformly conserved amino acids other than the two cysteines and two histidines [7–10]. Rieske-type proteins include bacterial ferredoxins, oxygenases, and their homologs [7–9,11,12]. In eukaryotic species, two Rieske-type proteins, CMP-N-acetylneuraminic acid hydroxylase (CMAH) and Neverland, have homology to bacterial oxygenases and, like AIFL, contain a ligand binding site that can accommodate a [2Fe–2S] cluster. CMAH is responsible for Neu5Gc biosynthesis [13], and Neverland is involved in ecdysone synthesis [14].

Abbreviations: AIF, apoptosis inducing factor; AMID, apoptosis-inducing factor-homologous mitochondrion-associated inducer of death; AIFL, apoptosis inducing factor-like; Pyr_redox, pyridine nucleotide-disulfide oxidoreductase; PRG3, p53-responsive gene 3.

* Corresponding author. Fax: +81 4 7136 3663.
E-mail addresses: 97318@ib.k.u-tokyo.ac.jp (Y. Murata), mitani@k.u-tokyo.ac.jp (H. Mitani).

0006-291X/$ - see front matter © 2011 Elsevier Inc. All rights reserved.
doi:10.1016/j.bbrc.2011.02.115

We found that in medaka (*Oryzias latipes*), a major isoform of AIFL that lacks the Pyr_redox domain (designated AIFL-I4) is translated from an AIFL transcript that retained intron 4. This report is the first to demonstrate the nuclear localization of a Rieske-type protein lacking a Pyr_redox domain produced by an AIFL gene, and our data showed that the [2Fe–2S] cluster binding site was essential for the nuclear localization of AIFL-I4 and was necessary for changes in mitochondrial morphology and suppression of cell proliferation.

2. Materials and methods

2.1. Fish breeding and temperature treatment

The orange-red strain of medaka (*O. latipes*) was maintained at 26 °C under a 14/10 h light/dark cycle. Embryos were maintained at 28 °C under a 14/10 h light/dark cycle. Developmental stages were determined according to Iwamatsu's developmental staging [15].

2.2. Sequencing of medaka AIFL transcripts

To identify the medaka genomic region containing the homolog to the human AIFL gene (GeneBank Accesion No. BC032485), medaka genome sequence was sequenced and analyzed using the UTGB database (http://utgenome.org/UTGBMedaka/). The medaka AIFL intron/exon boundary was estimated using GENSCAN (http://genes.mit.edu/GENSCAN.html) and alignment with the *Takifugu* genome sequence [16]. Full-length AIFL (fAIFL) transcripts from cultured medaka cell line (OLCAB-e3) [17] were amplified from 5′ to 3′ UTR using primers with sequences of 5′-TGG CAC CCC TCA CTC CTG-3′ and 5′-GTG GGT CCT TCT GAA GCT GT-3′ over 35 cycles (94 °C for 30 s, 65.7 °C for 30 s, and 72 °C for 90 s). The amplified product was cloned into pCR 4-TOPO (Invitrogen, CA, USA) and sequenced with the BigDye Terminator ver. 3.1 Cycle Sequencing kit (Applied Biosystems, CA, USA) using the primers used for PCR amplification.

2.3. Quantification of fAIFL and AIFL-I4 transcripts

Total RNA was extracted from the mature males (liver, muscle, intestine, brain, and testis), embryos (stages 25, 33, and 36) and OLCABe3 cells with ISOGEN (Nippon Gene, Tokyo, Japan) according to the manufacturer's instructions. The RNA was subjected to genome DNA degradation and RNA purification using an RNase-free DNase kit and an RNeasy® MinElute® Cleanup kit (Qiagen, Tokyo, Japan), respectively, according to the manufacturer's protocols. First-strand cDNA was synthesized with ReverTra Ace-α™ system (Toyobo, Osaka, Japan) following the manufacturer's instructions. Relative expression of fAIFL and AIFL-I4 were evaluated by quantitative real-time PCR (qRT-PCR) using SYBR® Premix Ex Taq (TaKaRa, Shiga, Japan) with a Smart Cycler II system (Cepheid, Sunnyvale, CA) following the manufacturer's instructions. All relative mRNA levels analyzed in qRT-PCR were normalized with β-actin and also with the intestine. The following primer sequences were used for qRT-PCR amplifications of fAIFL from exons 3 to 5 (forward 5′-GGT CAA AGG TGT GCT GTC AA-3′ and reverse 5′-AGA CCG GAC AGG ACC AAC AG-3′), AIFL-I4 from exon 3 to intron 4 (forward 5′-GGT CAA AGG TGT GCT GTC AA-3′ and reverse 5′-AAC TCT GAC CTG GAA GAC GG-3′) and β-actin (forward 5′-CAC TCT GAG CGC CGT CAC ACA CAG-3′ and reverse 5′-TGA CAC CCT GGT GCC TGG GGC GAC-3′).

2.4. Heat induction of fAIFL and AIFL-I4

For the heat induction, the medaka HSP70.1 promotor was subcloned into the *Nhe*I and *Xho*I sites of pGL4.22 plasmid (Promega, Madison, WI) after PCR amplification of pG-olphsp70.1-hRluc-Venus by primers with the *Nhe*I site on the 5′-end and the *Xho*I site on the 3′-end [18]. The Venus gene, a YFP variant, was fused to the 3′-end of the fAIFL and AIFL-I4 cDNAs and cloned into the *Xho*I site of pGL4.22 after PCR amplification of the Venus cDNA using primers to insert the *Xho*I site on the 5′-end and the *Eco*RI site on the 3′-end. The fAIFL and AIFL-I4 cDNAs were also cloned into the *Xho*I and *Eco*RI sites of pGL4.22 for comparing to fAIFL- and AIFL-I4-Venus. The 109th cysteine of AIFL-I4, a binding site for a [2Fe–2S] cluster, was converted to alanine using Genetailor (Invitrogen), according to the manufacturer's instructions.

2.5. Cell culture, transfection, and establishment of cell lines

OLCAB-e3 cells were grown at 33 °C in L-15 medium (Irvine Scientific, Santa Ana, CA) buffered with 10 mM 2-[4-(2-hydroxyethyl)-1-piperazinyl] ethanesulfonic acid (HEPES) and supplemented with 20% (v/v) fetal bovine serum (Nippon Bio-Supply Center, Tokyo, Japan) and 50 mg/ml streptomycin [17,19]. OLCAB-e3 cells were transformed with expression construct using a MicroPorator MP-100 (Digital Bio, Tokyo, Japan), and transformed cells were selected by adding puromycin (1 μg/ml) to the growth medium. fAIFL and AIFL-I4 expression from the transformed constructs was confirmed by fluorescence microscopy and western blotting after heat shock treatment (40 °C, 1 h).

2.6. Microscopy

Cell images were captured using an inverted light microscope (Olympus IX81, Tokyo, Japan). Red, green and blue images were captured sequentially using a highly sensitive DP-70 camera and DPcontroller software (Olympus). Mitochondria and nuclei in specimen samples were stained with MitoTracker® Red CM-H_2XROS (200 nM, 25 min, 33 °C, Molecular Probes) and Hoechst 33342 (200 ng/ml, 10 min, 33 °C, Wako). The total number of stained cells was counted using ImageJ software. The number of cells with mitochondria shorter than 5 μm was counted to estimate the change in mitochondrial morphology. Cells were stained with monoclonal anti-β-tubulin antibody produced in the mouse (Sigma–Aldrich, St. Louis, MO, USA) according to Hidaka et al. [20], and the percentages of mitotic cells that organized a spindle body were determined.

2.7. Statistics

The images and table entries are representative results from at least three independent experiments. To compare data from different treatment groups, we used the Student's *t*-tests to assess differences in mitochondrial morphology change rate and cell proliferation. Differences were considered statistically significant when $p < 0.05$. Results are presented as the mean ± SD for replicate experiments.

3. Results

3.1. Isolation of an alternative AIFL transcript

Sequencing of cDNAs representing AIFL transcripts containing exons 1–20 from the cultured medaka cell line (OLCAB-e3) showed several splicing variants. We conducted RT-PCR, and 30 amplification products were cloned into TOPO TA vectors. In all 30 clones,

exon 19 was spliced. fAIFL was encoded in 13 clones, and the other 17 clones encoded a transcript that retained intron 4 (Table 1). In embryos, the transcripts which contain exon 19 were also found. However, all introns of AIFL possessed the consensus splice sites in their 5′- and 3′-ends. The retention of intron 4 resulted in a change in the open reading frame that generated a stop codon. The resulting protein, designated AIFL-I4, was predicted to contain a Rieske domain, but lack a Pyr_redox domain (Fig. 1A).

3.2. Quantification of AIFL-I4 and fAIFL transcripts in adult tissues and embryos

cDNAs from adult medaka tissues (muscle, brain, intestine, testis, and liver), embryos (stages 25, 33, and 36), and OLCAB-e3 cells were examined by RT-PCR and qRT-PCR. We found that both AIFL-I4 and fAIFL transcripts were abundant in the brain and stage 36 embryos (Fig. 1B and Table 2). AIFL-I4 and fAIFL transcripts were more highly expressed in the brain, than in any samples, and expression levels were 301.22 ± 5.18 and 181.58 ± 14.51, respectively (Table 2). Expression levels of both AIFL-I4 and fAIFL transcripts increased through embryonic development (from stages 25 to 36); the relative amounts of expression of AIFL-I4 transcripts were 1.58 ± 0.26 to 16.43 ± 4.81, at stages 25 and 36, and those of fAIFL transcripts were 1.26 ± 0.17 to 30.13 ± 6.76 (Table 2).

3.3. AIFL-I4 localized to the nucleus and induced changes in mitochondrial morphology and suppression of cell proliferation

Xie et al. [2] reported that constitutive overexpression of human AIFL induced apoptosis in cultured human cell line. Therefore, we employed a medaka HSP70.1 promotor (*olphsp70.1*) [18] to transiently overexpress medaka fAIFL or AIFL-I4. Constructs encoding AIFL-I4-Venus or fAIFL-Venus [21] fusion protein driven under *olphsp70.1* were electro-transfected into OLCAB-e3 cells derived from embryos, and we established cell lines that transiently expressed each of the fusion proteins after heat shock treatment (40 °C, 1 h).

Western blot analysis with an anti-GFP antibody indicated that expression of AIFL-I4-Venus (46 kDa) and fAIFL-Venus (92 kDa) were actually induced by heat shock treatment in those cell lines; the expression of the fusion proteins was also confirmed by fluorescence microscopy (Supplemental figure, Fig. 2A and B). The cell lines expressing each the Venus fusion proteins and OLCAB-e3 cell line were observed for 24 h after heat shock treatment by time-lapse microscopy. After heat shock treatment, the induction of apoptotic cells was not found in any the cell lines (data not shown).

During 12 h of time-lapse fluorescence microscopic observation after heat shock treatment, AIFL-I4-Venus assembled around the nucleus and accumulated in the nucleus (Fig. 2B and Supplemental movie). In contrast, fAIFL-Venus was distributed throughout the cytosol (Fig. 2A). After 12 h, degradation of the fluorescence was found in both AIFL-I4-Venus and fAIFL-Venus cell lines. Therefore, we stained lysosomes of both the cell lines and found that AIFL-I4-Venus and fAIFL-Venus colocalized with lysosomes (data not shown). Over 24 h of time-lapse observation of cells overexpressing AIFL-I4-Venus, we observed an increase in the number cells with mitochondria less than 5 μm in length (Fig. 3A and B) and slight suppression of cell proliferation (data not shown). In AIFL-I4-Venus cell lines, the frequency of cells with changed mitochondrial morphology was significantly increased from 2.04 ± 0.49% (before heat shock treatment) to 13.54 ± 1.96% (8 h after heat shock treatment). In contrast, fAIFL-Venus-expressing cells showed normal tubular mitochondria and a normal cell proliferation rate after heat shock treatment (Fig. 3B). We next counted the number of cells undergoing mitosis using anti-β-tubulin antibody and Hoechest 33342 in about 1000 cells within 24 h after heat shock treatment. AIFL-I4-Venus cells showed a decreased number of cells in mitosis from 1% (before heat shock treatment) to 0.4% (24 h after heat shock treatment), while the number of mitotic fAIFL-Venus-expressing cells did not change after heat shock treatment (Table 3). Changes in mitochondria morphology and supression of cell proliferation were also confirmed after overexpression of AIFL-I4 without a Venus tag (data not shown).

Table 1
Types of AIFL transcripts in cultured medaka cell line (OLCAB-e3).

Splicing variant	Number of clones
fAIFL (exons 1–18 and exon 20)	13
AIFL-I4 (exons 1–4 retained intron 4, exons 5–18, and exon 20)	17
Total	30

3.4. A mutant AIFL-I4 with a non-functional [2Fe–2S] cluster binding site did not affect cell proliferation or mitochondria morphology

In Rieske proteins, the uniformly conserved four amino acids (Cys-X-His-X_{15-47}-Cys-X-X-His) are all essential for electron storage and transfer [22,23]. Rieske proteins and Rieske-type proteins may be derived from one common ancestor [9]. The amino acid sequence of AIFL-I4 is classified as a Rieske-type protein. We hypothesized that the four amino acids in Rieske-type proteins are also essential for their function, and that the Rieske domain is involved in the nuclear localization and functions of AIFL-I4. Thus, one of the ligands, the 109th cysteine in AIFL-I4, was converted to alanine and the mutant construct was electro-transferred into OLCAB-e3 cells. Established C109A-Venus cell lines showed cytosolic localization after heat shock treatment (Fig. 2C). The changes in mitochondrial morphology and suppression of cell proliferation that were induced by AIFL-I4-Venus expression were not observed (Fig. 3B and Table 2).

4. Discussion

Firmly established examples of intron retention in human transcripts have been reported, but their biological significance is still uncertain [24]. The retained introns may cause premature termination codons (PTCs), and the nonsense-mediated decay (NMD) pathway is thought to prevent the synthesis of truncated proteins that have potentially toxic effects, such as dominant negative interactions. However, full physiological importance and mechanisms of intron retention are not yet clear [25]. We searched for human and mouse orthologs of the medaka AIFL-I4 cDNA in the Ensembl genome browser (http://www.ensembl.org/index.html) and found a transcript lacking the Pyr_redox domain in humans (GenBank Accession No. BX428310). Therefore, studies of the stable expression of medaka AIFL-I4 transcripts in tissue-specific and stage-specific patterns could enhance understanding of NMD pathway and intron retention.

fAIFL and AIFL-I4 were transcribed abundantly in the brain (Fig. 1B and Table 2). This result was consistent with the results of human microarray analysis [26]. In *Xenopus*, *Nfrl* (one of the orthologs of human AIFL) transcripts are also expressed in the neuroectoderm in neurula [27]. These data suggested that fAIFL and AIFL-I4 have tissue-specific function. Relative amounts of AIFL-I4 transcripts to fAIFL were high in muscle, cultured cells, and stage 25 embryos, but low in brain, liver, and stage 36 embryos. These results suggested that fAIFL and AIFL-I4 expression levels were regulated in a tissue-specific manner. Exon 19 was spliced in AIFL transcripts from OLCAB-e3 sequences (Table 1), but fAIFL transcripts with and without exon 19 were also found in embryonic

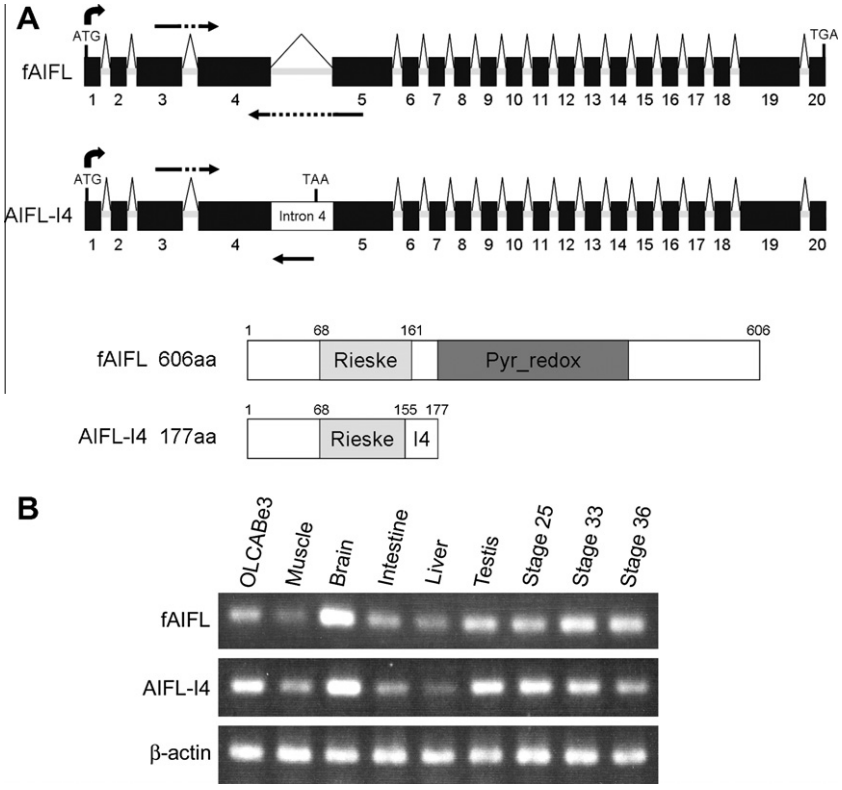

Fig. 1. Medaka AIFL gene structure and RT-PCR of fAIFL and AIFL-I4 transcripts from medaka adult tissues, embryos, and cultured cells. (A) In the AIFL genomic structure (top panel), black boxes represent constitutive exons, and gray boxes represent introns (not to scale). The translation start (ATG) and stop (TGA/TAA) codons are indicated, and the predicted domain structures are shown below. Numbers in the AIFL gene model designate exons and amino acids in the box model of the proteins. Arrows indicate schematic representation of the two primer pairs used in the quantification of fAIFL and AIFL-I4 transcripts. The retention of the 100-bp intron produces AIFL-I4, which lacks amino acids 156 through 606 of the full-length protein. AIFL-I4 retains the electron transfer domain (Rieske domain), but lacks the oxidoreductase domain (Pyr_redox domain). (B) Expression pattern of fAIFL and AIFL-I4 transcripts in multiple medaka tissues, embryos, and cultured cells using the designed primer pairs. β-actin was used as a loading control.

Table 2
Relative expression of fAIFL and AIFL-I4 by quantitative real-time PCR.

Tissues	fAIFL	AIFL-I4
OLCABe3	1.42 ± 0.35	8.20 ± 3.22
Muscle	3.20 ± 0.59	7.29 ± 0.81
Brain	301.22 ± 5.18	181.58 ± 14.51
Intestine	1 ± 0.22	1 ± 0.23
Testis	8.57 ± 2.30	11.79 ± 1.66
Liver	3.16 ± 0.34	2.24 ± 0.38
Muscle	3.20 ± 0.59	7.29 ± 0.81
Stage 25	1.26 ± 0.17	1.58 ± 0.26
Stage 33	8.94 ± 2.29	5.01 ± 1.37
Stage 36	30.13 ± 6.76	16.43 ± 4.81

All expression data were normalized by β-actin and standardized by intestinal levels. Mean ± SD for at least three experiments are presented.

cDNAs (data not shown). In fugu, stickleback, human and mouse, exon 19 is transcribed as one of the coding region, whereas exon 19-spliced transcripts are also reported in these species. It is indicated that a mechanism of splicing exon 19 of AIFL is conserved among these species. Splicing exon 19 of AIFL may be necessary for AIFL function, and a tissue-specific splicing system for exon 19, like that of intron 4, may exist.

Overexpression of AIF in mouse granule cells decreases peroxide-mediated cell death [28], and it is known that AIF plays a role as a radical scavenger via its putative oxidoreductase and peroxide scavenging activities [29]. fAIFL also contains the Pyr_redox domain, and the transcripts were abundant in medaka brain. Taken together, these results strongly suggest that fAIFL plays a role as a radical scavenger for proper development and maintenance of the nervous system in medaka nerve cells.

Schmidt et al. [9] proposed that both Rieske proteins and Rieske-type proteins are derived from a common ancestral gene. In Rieske proteins, the uniformly conserved four amino acids are all essential for electron storage and transfer [22,23]. Therefore, we conducted site-directed mutagenesis in one of the four amino acids, [2Fe–2S] cluster binding site, in AIFL-I4 and revealed that the mutagenesis prevented nuclear localization of AIFL-I4 (Fig 3C). This report is the first to demonstrate that AIFL-I4, Rieske-type proteins, was identified in the nucleus and the [2Fe–2S] cluster binding site was essential for nuclear localization. However, fAIFL did not localize to the nucleus. These findings suggest that the Pyr_redox domain inhibits some functions of the Rieske domain. Fe–S clusters are rare in nuclear enzymes but are present in some proteins [30,31]. It has been reported that two DNA repair glycosylases (MutY and endonuclease III) and DNA repair helicases (XPD and FancJ (also known as BACH1 and BRIP1)) contain a [3Fe–4S] cluster or [4Fe–4S] cluster [32,33]. Boal et al. [32] proposed that the base excision repair enzymes that contain the Fe-4S clusters become redox-active when they bound to DNA and redistribute rapidly onto genome sites in the vicinity of DNA lesions. MutY and endonuclease III may play a role in the rapid detection of DNA lesions using DNA-mediated electron transfer. Rudolf et al. [33] demonstrated that Fe–S clusters in XPD and FancJ are essential for helicase activity. AIFL-I4 may be involved in the detection of DNA damage or play another role with other proteins like helicase. In our case, overexpression and nuclear localization of AIFL-I4 may cause transcriptional aberrations due to AIFL-I4 binding to DNA and induced a change in mitochondrial morphology and the suppression of cell proliferation.

In this study, we have identified a major splicing variant of the AIFL gene that retained intron 4; this variant encodes AIFL-I4, a

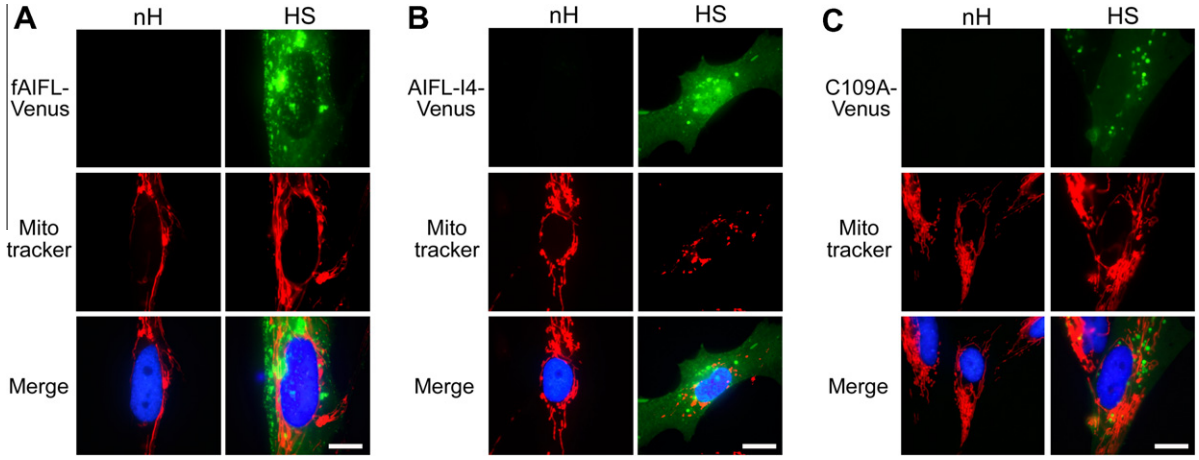

Fig. 2. Subcellular distribution of fAIFL, AIFL-I4 and C109A. (A–C) After 8 h of heat shock, subcellular distribution of the cell lines expressing fAIFL-Venus, AIFL-I4-Venus or C109A-Venus was observed. Cells were stained with the mitochondrial specific dye, Mitotracker, and the nucleus specific dye, Hoechest 33342. Mitotracker, Hoechest 33342, and Venus fusion proteins were visualized using fluorescence microscopy. fAIFL-expressing cells showed cytosol localization of the fusion protein, whereas AIFL-I4-expressing cells showed fusion protein localized to the nucleus, assembled around the nucleus, and in the cytosol (A and B (right)). C109A-expressing cells showed fusion protein did not localize to the nucleus (C (right)). nH, non heat shock; HS, heat shock. Bar, 10 μm.

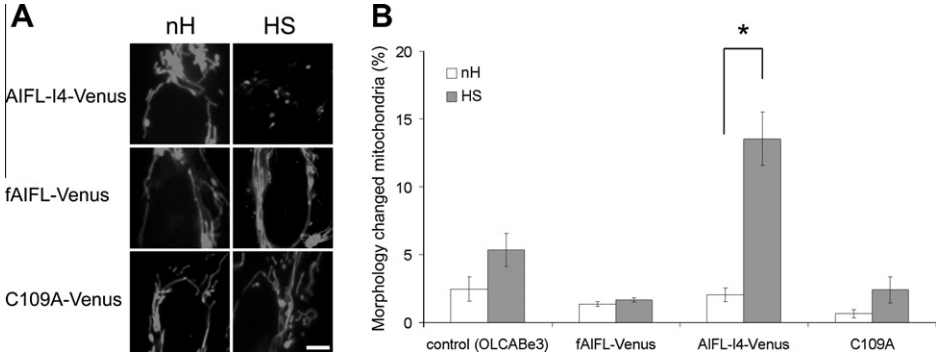

Fig. 3. Mitochondrial morphology in AIFL-I4-Venus- and fAIFL-Venus-expressing cells. (A) Magnified images of mitochondrial morphologies were taken from Fig. 2A–C. nH, no heat shock; HS, at 8 h after heat shock (40 °C, 1 h). Bar, 5 μm. (B) The graph shows the percentages of cells with morphologically-changed mitochondria in at least 100 cells from each cell line. The mitochondria in almost all of the wild-type cells were longer than 5 μm. Mean ± SD for three independent experiments are shown. $^{*}p < 0.05$.

Table 3
The number of mitotic cells in each cell line.

	nH			HS		
	Cell number	Division cell number	Division cell rate	Cell number	Division cell number	Division cell rate
OLCAB-e3	1147 ± 80	23 ± 2	2.0%	1108 ± 60	19 ± 5	1.7%
fAIFL-Venus	1158 ± 94	19 ± 5	1.6%	1074 ± 59	20 ± 4	1.9%
AIFL-I4-Venus	1124 ± 76	12 ± 1	1.1%	1135 ± 61	4 ± 2	0.4%
C109A-Venus	1029 ± 13	22 ± 3	2.1%	982 ± 55	23 ± 3	2.3%

nH, non heat shock; HS, heat shock. Mean ± SD for at least three independent experiments are presented.

novel Rieske-type protein. Nuclear localization of AIFL-I4 seemed to induce a change in mitochondrial morphology and suppression of cell proliferation, and the [2Fe–2S] cluster of AIFL-I4 was essential for nuclear localization. This report is the first to demonstrate nuclear localization of a Rieske-type protein. AIFL-I4 was abundantly expressed in the brain and may be involved in the embryonic development.

Acknowledgments

This study was supported by a Grant-in-Aid for Scientific Research (18310038 and 21221003) from the Ministry of Education, Culture, Sports, Science and Technology of Japan to H.M.

Appendix A. Supplementary data

Supplementary data associated with this article can be found, in the online version, at doi:10.1016/j.bbrc.2011.02.115.

References

[1] S.A. Susin, H.K. Lorenzo, N. Zamzami, et al., Molecular characterization of mitochondrial apoptosis-inducing factor, Nature 397 (1999) 441–446.
[2] Q. Xie, T. Lin, Y. Zhang, et al., Molecular cloning and characterization of a human AIF-like gene with ability to induce apoptosis, J. Biol. Chem. 280 (2005) 19673–19681.
[3] Y. Ohiro, I. Garkavtsev, S. Kobayashi, et al., A novel p53-inducible apoptogenic gene, PRG3, encodes a homologue of the apoptosis-inducing factor (AIF), FEBS Lett. 524 (2002) 163–171.

[4] M. Wu, L.G. Xu, X. Li, et al., AMID, an apoptosis-inducing factor-homologous mitochondrion-associated protein, induces caspase-independent apoptosis, J. Biol. Chem. 277 (2002) 25617–25623.
[5] N. Modjtahedi, F. Giordanetto, F. Madeo, G. Kroemer, Apoptosis-inducing factor: vital and lethal, Trends Cell Biol. 16 (2006) 264–272.
[6] D.J. Ferraro, L. Gakhar, S. Ramaswamy, Rieske business: structure-function of Rieske non-heme oxygenases, Biochem. Biophys. Res. Commun. 338 (2005) 175–190.
[7] J.R. Mason, R. Cammack, The electron-transport proteins of hydroxylating bacterial dioxygenases, Annu. Rev. Microbiol. 46 (1992) 277–305.
[8] T.A. Link, The structures of Rieske and Rieske-type proteins, Advances in Inorganic Chemistry, vol. 47, Academic Press Inc., San Diego, 1999, pp. 83–157.
[9] C.L. Schmidt, L. Shaw, A comprehensive phylogenetic analysis of Rieske and Rieske-type iron-sulfur proteins, J. Bioenerg. Biomembr. 33 (2001) 9–26.
[10] D. Kuila, J.A. Fee, Evidence for a redox-linked ionizable group associated with the [2Fe–2S] cluster of Thermus Rieske protein, J. Biol. Chem. 261 (1986) 2768–2771.
[11] E.L. Neidle, C. Hartnett, L.N. Ornston, et al., Nucleotide sequences of the *Acinetobacter calcoaceticus* benABC genes for benzoate 1,2-dioxygenase reveal evolutionary relationships among multicomponent oxygenases, J. Bacteriol. 173 (1991) 5385–5395.
[12] J. Castresana, M. Lubben, M. Saraste, New archaebacterial genes coding for redox proteins: implications for the evolution of aerobic metabolism, J. Mol. Biol. 250 (1995) 202–210.
[13] W. Schlenzka, L. Shaw, S. Kelm, et al., CMP-N-acetylneuraminic acid hydroxylase: the first cytosolic Rieske iron-sulphur protein to be described in Eukarya, FEBS Lett. 385 (1996) 197–200.
[14] T. Yoshiyama, T. Namiki, K. Mita, et al., Neverland is an evolutionally conserved Rieske-domain protein that is essential for ecdysone synthesis and insect growth, Development 133 (2006) 2565–2574.
[15] T. Iwamatsu, Stages of normal development in the medaka *Oryzias latipes*, Mech. Dev. 121 (2004) 605–618.
[16] S. Fukamachi, T. Yada, H. Mitani, Medaka receptors for somatolactin and growth hormone: phylogenetic paradox among fish growth hormone receptors, Genetics 171 (2005) 1875–1883.
[17] M. Hirayama, H. Mitani, S. Watabe, Temperature-dependent growth rates and gene expression patterns of various medaka *Oryzias latipes* cell lines derived from different populations, J. Comp. Physiol. B. 176 (2006) 311–320.
[18] S. Oda, S. Mikami, Y. Urushihara, et al., Identification of a functional medaka heat shock promoter and characterization of its ability to induce exogenous gene expression in medaka *in vitro* and *in vivo*, Zoolog. Sci. 27 (2010) 410–415.
[19] J. Komura, H. Mitani, A. Shima, Fish cell-culture: establishment of two fibroblast-like cell lines (OL-17 and OL-32) from fins of the medaka, *Oryzias latipes*, In Vitro cellular & development biology 24 (1988) 294–298.
[20] M. Hidaka, S. Oda, Y. Kuwahara, M. Fukumoto, H. Mitani, Cell lines derived from a medaka radiation-sensitive mutant have defects in DNA double-strand break responses, J. Radiat. Res. 51 (2010) 165–171.
[21] T. Nagai, K. Ibata, E.S. Park, et al., A variant of yellow fluorescent protein with fast and efficient maturation for cell-biological applications, Nat. Biotechnol. 20 (2002) 87–90.
[22] L.A. Graham, B.L. Trumpower, Mutational analysis of the mitochondrial Rieske iron-sulfur protein of *Saccharomyces cerevisiae*. III. Import, protease processing, and assembly into the cytochrome bc1 complex of iron-sulfur protein lacking the iron-sulfur cluster, J. Biol. Chem. 266 (1991) 22485–22492.
[23] J.R. Mason, C.S. Butler, R. Cammack, J.K. Shergill, Structural studies on the catalytic component of benzene dioxygenase from *Pseudomonas putida*, Biochem. Soc. Trans. 25 (1997) 90–95.
[24] Z. Kan, D. States, W. Gish, Selecting for functional alternative splices in ESTs, Genome Res. 12 (2002) 1837–1845.
[25] S. Brogna, J. Wen, Nonsense-mediated mRNA decay (NMD) mechanisms, Nat. Struct. Mol. Biol. 16 (2009) 107–113.
[26] A.I. Su, T. Wiltshire, S. Batalov, A gene atlas of the mouse and human protein-encoding transcriptomes, Proc. Natl. Acad. Sci. USA 101 (2004) 6062–6067.
[27] S. Hatada, M. Kinoshita, H. Sakumoto, et al., Novel gene encoding a ferredoxin reductase-like protein expressed in the neuroectoderm in *Xenopus neurula*, Gene 194 (1997) 297–299.
[28] J.A. Klein, C.M. Longo-Guess, M.P. Rossmann, et al., The harlequin mouse mutation downregulates apoptosis-inducing factor, Nature 419 (2002) 367–374.
[29] S. Krantic, N. Mechawar, S. Reix, R. Quirion, Apoptosis-inducing factor: a matter of neuron life and death, Prog. Neurobiol. 81 (2007) 179–196.
[30] C.F. Kuo, D.E. McRee, C.L. Fisher, et al., Atomic structure of the DNA repair [4Fe–4S] enzyme endonuclease III, Science 258 (1992) 434–440.
[31] J.A. Hinks, M.C. Evans, Y. De Miguel, et al., An iron-sulfur cluster in the family 4 uracil-DNA glycosylase, J. Biol. Chem. 277 (2002) 16936–16940.
[32] A.K. Boal, E. Yavin, O.A. Lukianova, et al., DNA-bound redox activity of DNA repair glycosylases containing [4Fe–4S] clusters, Biochemistry 44 (2005) 8397–8407.
[33] J. Rudolf, V. Makrantoni, W.J. Ingledew, et al., The DNA repair helicases XPD and FancJ have essential iron-sulfur domains, Mol. Cell 23 (2006) 801–808.